Reversible Information Hiding in Images Based on Histogram Shift Method

Min-Hao Wu,[1] Ting-Cheng Chang,[1*] Haishan Chen,[1] Zhenlun Yang,[1] and ShiMing Liu[2]

[1]School of Information Engineering, Guangzhou Panyu Polytechnic,
No. 1342, Shiliang Road, Panyu District, Guangzhou City, Guangdong Province 511483, China
[2]School of Management, Guangzhou Panyu Polytechnic,
No. 1342, Shiliang Road, Panyu District, Guangzhou City, Guangdong Province 511483, China

With the increasing popularity of wireless sensor networks in the IoT and Industry 4.0 era, the security of networks is critical in transmitting data and information. To address this need, we propose an optimized method for hiding and extracting information from image data. For this method, we created algorithms for hiding and extracting information based on the histogram shift method. The algorithms were developed using chessboard- and column-type prediction methods. Five different prediction methods were tested in the development of the algorithms, and the test results showed that the chessboard-type methods yielded better results with images. Then, the optimized prediction method was tested for various images along with previous methods. The results show that the proposed method has better results in terms of bits per pixel and peak signal-to-noise ratio. The method can be applied to image transmission through a wireless sensor network and provides a basis for the development of further applications.

1. Introduction

A wireless sensor network (WSN) is designed to collect data from numerous wireless sensors in different locations. In many cases, the data must be visualized as various images, which requires information hiding technology to ensure security.[1] Thus, reversible information hiding and file encryption have attracted much research interest for security in exchanging information in WSNs. Reversible information hiding is an ideal solution for high-fidelity content. It has been commonly used to recover carrier signals from images, multimedia content, and communication systems. Reversible information hiding requires data concealing techniques, which have been extensively researched. In reversible information hiding, several processes are necessary: hiding, copyright recognition, tampering recovery, and retrieval. All the steps are carried out by a well-designed algorithm. However, hiding information may distort the original information, causing the recovered information to be altered. Therefore, various methods for the complete retrieval of hidden information, such as distortion-free compression, differential expansion,[2,3] histogram shift,[4,5] block segmentation,[6] pixel differentiation,[7] different growth,[8,9] and recursive coding[10] methods, have been proposed.

However, in many applications, the distortion metrics are position-dependent, which produces inconsistent results. Inconsistent distortion makes images easily embedded with confidential information that is difficult to recover. Under a multi-distortion index, the rate-distortion problem of reversible information hiding is undesirable. Thus, a basic framework for estimating and matching the optimum matrix is required. In this study, we propose a new histogram shift method based on the optimum hiding method. Referring to Sachnev *et al.*,[11] a method for the optimal hiding of the difference of values from the original data was developed. The proposed method with two different techniques carries out a multilevel hiding strategy for high-quality images.

2. Methods

2.1 Hiding information

We developed a new histogram shift method based on the optimum hiding method of Sachnev *et al.*[11] The method is divided into two types (Fig. 1): column type and chessboard type. In the column type, the algorithm hides information in the upper and lower cells or the right and left cells in the same column or row, respectively, while in the chessboard type, information is hidden diagonally in the upper right and bottom left cells or in the upper left and bottom right cells (Fig. 2). These methods are used to enhance the hiding capacity by avoiding
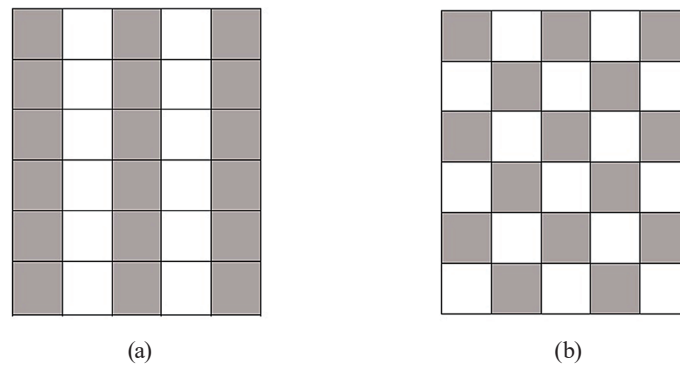

Fig. 1.   Two different types of histogram shift method. (a) Column type. (b) Chessboard type.
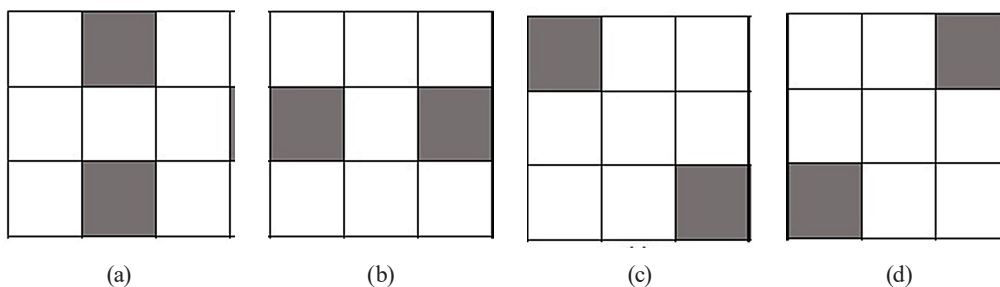

Fig. 2.   Two ways of hiding information in cells. (a, b) Column type. (c, d) Chessboard type.

the undistorted original data. In the chessboard type, the cells in which information is hidden match the moves of a pawn, while in the column type, the cells in which information is hidden match the moves of a bishop. Each pixel value is predicted using the average value of surrounding pixels. The pixel value is divided into two parts. Only the exact part is predicted each time, with the first prediction in the black part. The average value of the surrounding pixels is used to predict the error value of the black part. When all pixel error values are calculated, the numbers of occurrences of pixel error values are counted in a histogram. The first step finds the two most frequent highs and their relative zeros in the histogram. The second step uses displacement to hide confidential information in the image. In the third step, if all hidden pixel values are hidden, the inverse operation is used to obtain a camouflaged image with hidden secret information. Personal information must be hidden. The information-hiding steps are completed until all confidential information is hidden in the image.

2.2 Histogram shifting

To hide information in neighboring cells by histogram shifting, the indices of the peak value and zero must be defined. The histogram is created using the value differences of adjacent pixels. Then, the indices of the histograms have a peak (maximum) and zero value. The histogram with a certain range of indices is shifted to increase the value difference of all adjacent cells in the range by one. The peak value is adjusted to zero to embed data in the peak and neighboring cells.[12] As a result, the original peak value disappears in the histogram. Shifting the histogram allows underflow or overflow to be avoided when hiding information.[6]

2.3 Hiding algorithm

A simple prediction algorithm is described as follows. The algorithm places the peak value in the top cell and its vertically adjacent cell in column-type information hiding. Assuming that a cover image is an $m \times n$ gray cover image, $I_{i,j}$ denotes the pixel values before histogram shifting, $K_{i,j}$ is the overflow or underflow value, and $K'_{i,j}$ denotes the pixel values of the embedded image data after being refined at location (i, j). If the regularity of each pixel value is less than 10000, the image data is 'natural'. When the image is natural, we can assign a cell with the peak factor (the ratio of the maximum value to the root mean square value) and the cell to the left with the peak point to hide data. The peak point t is suitable for the peak factor, while the cell to the left is unsuitable. When the image is a medical image, we make one the highest of the peak point. The algorithm to assign cells with the peak factor and peak points is created as below. The output is a steganographic image K'.

Step 1. Input the cover image $I = \{I_{0,0}, I_{0,1}, ..., I_{0,n-1}, ..., I_{1,0}, ..., I_{m-1,n-1}\}$.
Step 2. Check each pixel value.
　　　　　If $p(i) < 10000$, then the image is a natural image.
　　　　　Else the image is a medical image,
　　　　　where $i \in (0, 255)$.

Step 3. Predict each pixel $K_{i,j}$ in the cover image and create prediction error value $e_{i,j}$ of linear predictor as follows:
   (a) If $i \neq 0$ and $j = 0$, then $e_{i,j} = K_{i,j} - K_{i+1,j+1}$.
   (b) Else $i \neq 0$ and $j \% 2 = 0$, then $e_{i,j} = K_{i,j} - \text{int(average } (K_{i-1,j-1}, K_{i+1,j+1}))$.

Step 4. Create histogram $h(x)$ from all predictive error values $e_{i,j}$, where $x \in (-255, 255)$.

Step 5. Find the peak and zero points as follows:
   If the image is a natural image, then find two pairs of peak and zero points (P_1, Z_1) and (P_2, Z_2) satisfying $Z_2 < P_2 < P_1 < Z_1$.
   Else find one peak and zero pair (P_1, Z_1) satisfying $P_1 < Z_1$.

Step 6. Shift the histogram as follows:
   If the image is a natural image, then
   (a) $e'_{i,j}$ is set to $e_{i,j} + 1$ if $e_{i,j} \in (P_1 + 1, Z_1 - 1)$,
   (b) $e'_{i,j}$ is set to $e_{i,j} - 1$ if $e_{i,j} \in (Z_2 + 1, P_2 - 1)$.
   Else $e'_{i,j}$ is set to $e_{i,j} + 1$ if $e_{i,j} \in (P_1 + 1, Z_1 - 1)$.

Step 7. Embed a medical record of illness as follows:
   If the image is a natural image, then
   (a) If the bit to be embedded is 0, $e'_{i,j}$ is set to $e_{i,j}$,
   (b) If the bit to be embedded is 1, $e'_{i,j}$ is set to $e_{i,j} + 1$ and $e_{i,j} - 1$,
   when $e_{i,j}$ is equal to P_1 and P_2, respectively.
   Else (a) If the bit to be embedded is 0, $e'_{i,j}$ is set to $e_{i,j}$,
       (b) If the bit to be embedded is 1, $e'_{i,j}$ is set to $e_{i,j} + 1$.

Step 8. Convert each embedded predictive error value $e'_{i,j}$ into its embedded pixel value.
   (a) If $i \neq 0$ and $j = 0$, then $K'_{i,j} = e'_{i,j} + K_{i+1,j+1}$.
   (b) If $i \neq 0$ and $j \% 2 = 0$, then $K'_{i,j} = e'_{i,j} + \text{int(average}(K_{i-1,j-1}, K_{i+1,j+1}))$.

Step 9. Predict each pixel $K_{i,j}$ in the cover image and create prediction error value $e_{i,j}$ of linear predictor as follows:
   (a) If $i \neq 0$ and $j \% 2 = 1$, then $e_{i,j} = K_{i,j} - \text{int(average}(K_{i-1,j-1}, K_{i+1,j+1}))$.
   (b) Else $i \neq 0$ and $j = 511$, then $e_{i,j} = K_{i,j} - K_{i-1,j-1}$.

Step 10. Create histogram h(x) from all predictive error values $e_{i,j}$, where $x \in (-255, 255)$.

Step 11. Find the peak and zero points as follows:
   If the image is a natural image, then find two pairs of peak and zero points (P_3, Z_3) and (P_4, Z_4) satisfying $Z_4 < P_4 < P_3 < Z_3$.
   Else find one peak and zero pair (P_3, Z_3) satisfying $P_3 < Z_3$.

Step 12. Shift the histogram as follows:
   If the image is a natural image, then
   $e'_{i,j}$ is set to $e_{i,j} + 1$ if $e_{i,j} \in (P_3 + 1, Z_3 - 1)$,
   $e'_{i,j}$ is set to $e_{i,j} - 1$ if $e_{i,j} \in (Z_4 + 1, P_4 - 1)$.
   Else $e'_{i,j}$ is set to $e_{i,j} + 1$ if $e_{i,j} \in (P_3 + 1, Z_3 - 1)$.

Step 13. Embed a medical record of illness as follows:
   If the image is a natural image, then
   (a) If the bit to be embedded is 0, $e'_{i,j}$ is set to $e_{i,j}$,
   (b) If the bit to be embedded is 1, $e'_{i,j}$ is set to $e_{i,j} + 1$ and $e_{i,j} - 1$.

when $e_{i,j}$ is equal to P_1 and P_2, respectively.

Else (a) If the bit to be embedded is 0, $e'_{i,j}$ is set to $e_{i,j}$,

(b) If the bit to be embedded is 1, $e'_{i,j}$ is set to $e_{i,j} + 1$.

Step 14. Convert each embedded predictive error value $e'_{i,j}$ into its embedded pixel value.

(a) If $i \neq 0$ and $j \% 2 = 0$, then $K''_{i,j} = e'_{i,j} + \text{int(average } (K_{i-1,j-1}, K_{i+1,j+1}))$.

(b) Else $i \neq 0$ and $j = 511$, then $K''_{i,j} = e'_{i,j} + K_{i-1,j-1}$.

Step 15. Output steganographic image K'' and sequence of optimum hiding s and peak and zero points.

2.4 Extraction algorithm

The embedded data expressed in the steganographic image K'' is extracted by reversing the hidden data from the pixel values. The extraction and reverse algorithm is as follows.

Step 1. Process each pixel of steganographic image K'' from left to right and then from top to bottom by following Step 3 to Step 5 repeatedly.

Step 2. Check each pixel value.

If $p(i) < 10000$, then the image is a natural image.

Else the image is a medical image,

where $i \in (0, 255)$.

Step 3. Predict each pixel $K_{i,j}$ in the cover image and create prediction error value $e_{i,j}$ of linear predictor as follows:

(a) If $i \neq 0$ and $j = 0$, then $e_{i,j} = K_{i,j} - K'_{i+1,j+1}$.

(b) Else $i \neq 0$ and $j \% 2 = 0$, then $e_{i,j} = K'_{i,j} - \text{int(average}(K'_{i-1,j-1}, K'_{i+1,j+1}))$.

Step 4. If the image is a natural image, then

Use the two pairs of peak and zero points (P_3, Z_3) and (P_4, Z_4) to extract the medical record and recover the prediction difference value into pixel values.

Else

Use the pair of peak and zero points (P_3, Z_3) to extract the medical record and recover the prediction difference value into pixel values.

Step 5. Predict each pixel $K_{i,j}$ in the cover image and create prediction error value $e_{i,j}$ of linear predictor as follows:

(a) If $i \neq 0$ and $j \% 2 = 1$, then $e_{i,j} = K_{i,j} - \text{int(average } (K_{i-1,j-1}, K_{i+1,j+1}))$.

(b) Else $i \neq 0$ and $j = 511$, then $e_{i,j} = K_{i,j} - K_{i-1,j-1}$.

Step 6. If the image is a natural image, then

Use the two pairs of peak and zero points (P_1, Z_1) and (P_2, Z_2) to extract the medical record and recover the prediction difference value into pixel values.

Else

Use the pair of peak and zero points (P_1, Z_1) to extract the medical record and recover the prediction difference value into pixel values.

Step 7. Output the original image and the medical record.

2.5 Prediction algorithm

For the reversibility of the proposed algorithms, a prediction algorithm is required to predict the difference of the retrieved data from the original data. The difference must be adjusted for the reversible information hiding process. In this study, we created an algorithm based on chessboard- and column-type information hiding. In the chessboard type, two prediction algorithms are used from the top cells to the bottom cells, while the second prediction method uses cells from the left to the right. The prediction algorithm carries out several interrelated actions at each stage for the optimized extraction of the hidden information. In this study, the algorithm was created with five different methods to find the ideal peak signal-to-noise ratio (PSNR).

3. Experimental Results

The proposed method is designed to ensure that the value difference of the cells in the steganographic image remains within ±1 to maintain the quality of the original image. The image quality is defined with PSNR, which pertains to a quality comparison between the original and hidden data. The higher the value of PSNR, the higher the quality of the hidden and extracted data. PSNR is defined as

$$PSNR = 10 \times \log_{10} \left(\frac{255^2}{MSE} \right),$$ (1)

where the mean square error (MSE) is calculated as

$$MSE = \frac{1}{m \times n} \left(\sum_{i=0}^{m} \sum_{j=0}^{n} I(i,j) - K(i,j) \right)^2.$$ (2)

Figure 3 shows the six grayscale images used in the experiment. We used 512 × 512 grayscale medical images in the experiment, which were obtained from computer tomography (CT) and magnetic resonance imaging (MRI).

3.1 Chessboard- and column-type prediction methods

The bits per pixel (BPP) and PSNR of the aircraft image [Fig. 3(a)] were compared for different prediction algorithms. Each prediction algorithm chooses the optimal way of extracting data with the best PSNR. Five prediction methods were tested in the prediction algorithm, which were named CHLR, CHUB, COLR, COURBL, and COULBR. Among the chessboard-type methods, CHLR hides and extracts data from the left and right cells of the original cell, and CHUB from the upper and lower cells. Among the column-type methods, COLR hides and
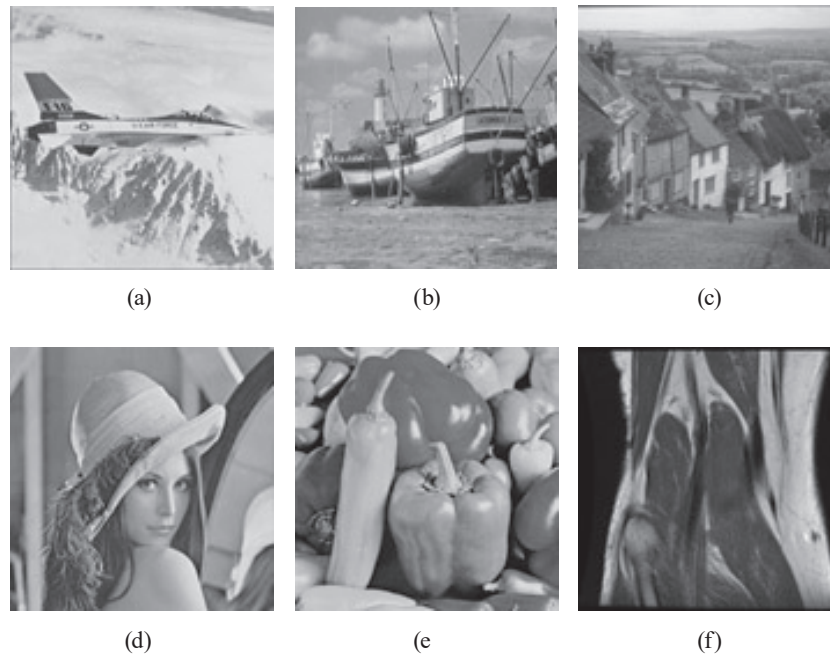
Fig. 3.   Six images used in the experiment. (a) Airplane. (b) Boat. (c) Goldhill. (d) Lena. (e) Peppers. (f) Sailboat.

Table 1
Comparison of BPP and PSNR of the aircraft image [Fig. 3(a)] for different prediction algorithms at different levels.

Level	Optimum program prediction		CHUB		CHLR		COLR		COURBL		COULBR	
	BPP	PSNR	BPP	PSNR	BPP	PSNR	BPP	PSNR	BPP	PSNR	BPP	PSNR
1	0.37	49.02	0.37	49.02	0.35	48.99	0.35	48.30	0.29	43.59	0.30	44.17
2	0.62	44.19	0.57	43.90	0.55	43.99	0.54	43.17	0.46	40.56	0.46	40.68
3	0.81	41.12	0.72	40.53	0.69	40.87	0.69	40.32	0.59	38.29	0.59	38.32
4	0.95	37.84	0.84	38.02	0.81	38.09	0.81	37.66	0.70	36.19	0.69	36.31
5	1.06	35.89	0.94	36.53	0.92	36.41	0.92	35.91	0.79	35.09	0.78	34.99
6	1.16	34.28	1.03	35.08	1.00	34.94	1.00	34.41	0.87	33.80	0.86	33.73
7	1.25	32.98	1.10	33.93	1.08	33.77	1.08	33.34	0.93	32.64	0.94	32.81
8	1.33	32.18	1.17	32.94	1.15	32.93	1.15	32.42	0.99	31.87	1.00	31.96
9	1.41	31.29	1.24	31.99	1.21	31.87	1.21	31.46	1.05	30.99	1.05	31.12
10	1.48	30.56	1.29	31.02	1.27	31.14	1.26	30.60	1.10	30.09	1.10	30.36
11	1.54	29.86	1.35	30.19	1.32	30.42	1.32	29.84	1.15	29.36	1.14	29.51
12	1.60	29.40	1.39	29.48	1.36	29.72	1.36	29.03	1.20	28.78	1.19	28.90

extracts data from the left two cells, COURBL from the upper and lower cells, and COULBR from the right two cells. Table 1 shows a comparison of BPP and PSNR for each method. The optimized prediction algorithm chose the best values of BPP and PSNR at each level of prediction. At the first level of prediction, the values selected for each method are the largest BPP and PSNR, which were selected for the optimized prediction method.

Table 2 presents the BPP and PSNR of the baboon image for each prediction method.[13] When PSNR is around 30, optimum hiding and extraction are enabled at the 10th level. For a complex image such as the baboon image, CHLR is regarded as the optimal method. The images extracted by CHUB and COLR have better BPP and PNSR values than those extracted by the other methods.

Table 3 shows a comparison of the BPP and PSNR of medical image M1 [Fig. 4(a)] for each prediction method. When PSNR is around 30, optimal prediction is enabled at the 16th level with BPP of 2.74. The chessboard-type methods CHUB and CHLR show better results than the

Table 2
Comparison of BPP and PSNR of the baboon image[13] for different prediction algorithms at different levels.

Level	Optimum program prediction		CHUB		CHLR		COLR		COURBL		COULBR	
	BPP	PSNR	BPP	PSNR	BPP	PSNR	BPP	PSNR	BPP	PSNR	BPP	PSNR
1	0.15	48.48	0.09	48.32	0.15	48.48	0.15	41.30	0.07	41.06	0.07	40.45
2	0.27	43.06	0.16	42.84	0.27	43.06	0.27	37.36	0.14	38.11	0.14	38.06
3	0.37	39.93	0.22	39.78	0.37	39.93	0.37	36.17	0.20	36.59	0.19	36.30
4	0.46	37.80	0.27	37.29	0.46	37.80	0.45	35.26	0.25	35.02	0.24	34.84
5	0.53	36.09	0.32	35.61	0.53	36.09	0.53	34.04	0.29	33.72	0.28	33.53
6	0.60	34.60	0.37	34.24	0.60	34.60	0.59	32.76	0.33	32.74	0.32	32.68
7	0.66	33.13	0.41	32.80	0.66	33.13	0.65	31.82	0.37	31.72	0.36	31.64
8	0.72	31.95	0.44	31.71	0.72	31.95	0.71	30.96	0.40	30.87	0.39	30.78
9	0.78	31.05	0.48	30.82	0.78	31.05	0.76	30.46	0.43	29.97	0.42	29.95
10	0.83	30.36	0.51	29.92	0.83	30.31	0.81	29.57	0.46	29.24	0.45	29.22
11	0.87	29.68	0.54	29.24	0.87	29.52	0.86	28.87	0.49	28.48	0.48	28.46

Table 3
Comparison of BPP and PSNR of medical image M1 [Fig. 4(a)] for different prediction algorithms at different levels.

| Level	Optimum program prediction		CHUB		CHLR		COLR		COURBL		COULBR	
	BPP	PSNR	BPP	PSNR	BPP	PSNR	BPP	PSNR	BPP	PSNR	BPP	PSNR
1	0.66	52.26	0.66	52.26	0.39	53.80	0.40	58.34	0.64	52.18	0.64	52.17
2	1.05	47.46	1.00	47.00	0.86	48.18	1.06	48.97	0.97	33.08	0.97	33.37
3	1.34	43.85	1.19	44.67	1.15	44.91	1.40	34.36	1.15	31.21	1.16	31.27
4	1.51	41.78	1.40	41.84	1.40	42.01	1.59	34.73	1.35	31.06	1.36	31.04
5	1.67	39.96	1.55	39.84	1.54	40.05	1.81	33.33	1.50	31.18	1.50	31.15
6	1.80	38.43	1.66	38.60	1.68	38.23	1.95	32.51	1.60	30.25	1.61	30.33
7	1.94	36.98	1.79	37.04	1.81	37.18	2.07	32.28	1.72	29.85	1.73	29.95
8	2.05	35.86	1.87	35.80	1.92	36.00	2.17	31.52	1.80	29.79	1.81	29.87
9	2.18	35.15	1.96	34.57	2.02	35.15	2.30	31.00	1.88	29.53	1.89	29.40
10	2.27	34.21	2.04	33.59	2.10	34.19	2.39	30.61	1.95	28.78	1.96	28.98
11	2.38	33.75	2.12	32.63	2.18	33.87	2.46	30.07	2.02	28.82	2.03	28.81
12	2.47	32.82	2.19	31.82	2.28	32.85	2.56	29.46	2.08	28.26	2.09	28.44
13	2.54	32.12	2.26	30.94	2.35	32.18	2.62	29.02	2.14	27.78	2.15	28.10
14	2.62	31.29	2.32	30.68	2.42	31.34	2.69	28.59	2.20	27.68	2.22	27.78
15	2.68	30.81	2.37	30.06	2.48	30.60	2.75	28.14	2.25	27.15	2.27	27.32
16	2.74	30.09	2.43	29.41	2.54	30.00	2.80	27.79	2.31	26.74	2.32	26.98
17	2.80	29.70	2.48	29.00	2.59	29.72	2.86	27.34	2.35	26.64	2.37	26.71
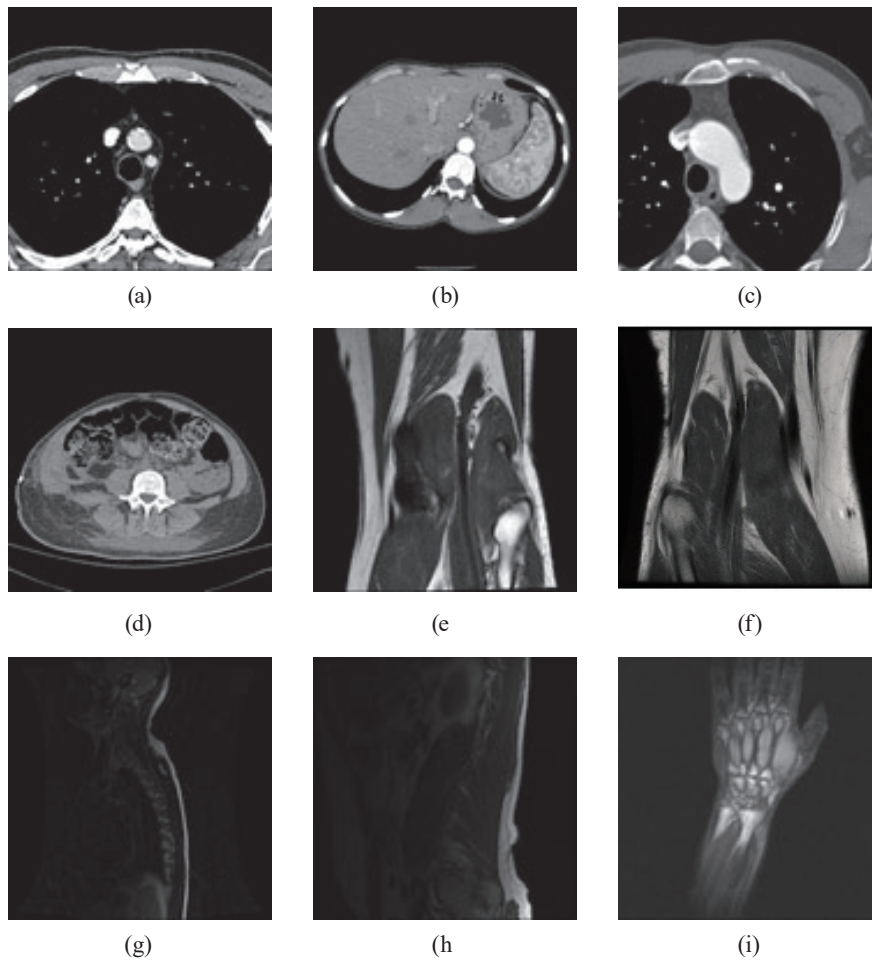
Fig. 4.   Nine medical images used in the experiment. (a)–(d) CT images; (e)–(i): MRI images. (a) M1, (b) M2, (c) M3, (d) M4, (e) M5, (f) M6, (g) M7, (h) M8, and (i) M9.

column-type methods COURBL and COULBR for the image. For PSNR of around 30, COURBL and COULBR show the best results at the 7th level.

Table 4 shows a comparison of BPP and PSNR of medical image M7 [Fig. 4(g)] for each prediction method. Optimized values of BPP and PSNR are found at the 6th level. The chessboard-type methods CHUB and CHLR show better results than the other column-type methods; among the column-type methods, COLR shows the best result but is still inferior to those of the chessboard-type methods.

3.2   Comparison with previous methods

The performance of the optimized prediction method in this study was compared with those of previous methods. Table 5 shows the BPP and PSNR of the hidden and extracted images for the methods of Ni *et al*.,[12] Tai *et al*.,[14] and Li *et al*.[7] and the proposed method. The results show that BPP for the proposed method is 8−26% higher than those for the other methods and PSNR is improved to 48.80, which is higher than that for the other methods. The chessboard-

Table 4
Comparison of BPP and PSNR of medical image M7 [Fig. 4(g)] for different prediction algorithms at different levels.

Level	Optimum program prediction		CHUB		CHLR		COLR		COURBL		COULBR	
	BPP	PSNR	BPP	PSNR	BPP	PSNR	BPP	PSNR	BPP	PSNR	BPP	PSNR
1	0.24	52.86	0.10	54.89	0.24	52.86	0.25	36.73	0.21	34.49	0.21	34.51
2	0.51	47.84	0.47	47.86	0.49	47.14	0.49	34.66	0.43	34.01	0.42	34.09
3	0.74	43.85	0.65	44.03	0.67	43.23	0.67	34.41	0.59	33.69	0.58	33.88
4	0.91	41.24	0.79	41.26	0.79	40.61	0.79	33.43	0.69	32.82	0.68	33.21
5	1.04	39.14	0.90	39.06	0.90	38.52	0.90	32.53	0.77	32.32	0.76	32.62
6	1.16	37.51	1.00	37.35	0.99	37.19	1.00	32.02	0.85	31.84	0.84	32.18
7	1.26	36.08	1.09	35.81	1.08	35.76	1.09	31.63	0.93	31.24	0.91	31.71
8	1.35	34.87	1.18	34.56	1.17	34.75	1.18	31.00	1.00	30.69	0.98	31.04
9	1.43	33.79	1.28	33.38	1.25	33.57	1.26	30.51	1.06	30.26	1.03	30.41
10	1.51	32.84	1.35	32.65	1.33	32.55	1.33	29.94	1.11	29.64	1.08	29.86
11	1.58	31.97	1.42	31.74	1.40	31.67	1.41	29.45	1.15	29.21	1.12	29.31
12	1.65	31.14	1.48	30.89	1.46	30.83	1.47	28.83	1.20	28.75	1.16	28.72
13	1.71	30.47	1.54	30.04	1.51	30.00	1.52	28.30	1.24	28.16	1.20	28.38
14	1.77	29.70	1.59	29.24	1.56	29.43	1.57	27.88	1.28	27.75	1.23	27.86

Table 5
Comparison of BPP and PSNR among different methods.

Image		Ni *et al.*[12]	Tai *et al.*[14]	Li *et al.*[7]	Proposed method
	Airplane	0.07	0.25	0.3	0.37
	Boat	0.04	0.17	0.19	0.26
	Goldhill	0.02	0.13	0.19	0.24
BPP	Lena	0.02	0.18	0.23	0.38
	Peppers	0.02	0.18	0.24	0.35
	Sailboat	0.03	0.12	0.14	0.15
	Average BPP	0.03	0.17	0.21	0.29
Average PSNR		48.3	48.79	48.47	48.80

type prediction algorithm was used for all images except Goldhill [Fig. 3(c)], which was hidden and extracted by the column-type algorithm.

Table 6 shows a comparison of the performance of the proposed algorithm with those of Fallahpour *et al.*'s three algorithms (GAP, Jiang, and MED). Except for the image of Goldhill, the images are hidden and extracted using the chessboard-type image. Compared with the three algorithms of Fallahpour *et al.*, the proposed method has an 8−10% higher BPP, but the PSNR of the proposed method is similar to those of the other algorithms.

Table 7 shows a comparison of the results of the methods of Sachnev *et al.*,[11] Lee *et al.*,[15] and Zhao *et al.*[16] and the proposed method. In the medical images, there were many under- and overflows, which increased the computational load. The methods of Sachnev *et al.*[11] and Lee *et al.*[15] can deal with such an additional computational load, but that of Zhao *et al.*[16] shows underflows, which increased its computational load by 3%. The proposed method shows a much lower BPP and fewer overflows and an improved PSNR.

Table 6
Comparison of BPP and PSNR for the algorithms of Fallahpour *et al.*[13] and the proposed method.

Image	GAP		Jiang		MED		Our method	
	BPP	PSNR	BPP	PSNR	BPP	PSNR	BPP	PSNR
Baboon	0.07	48.50	0.07	48.83	0.07	48.30	0.15	48.48
Barbara	0.18	49.00	0.17	48.50	0.17	48.55	0.20	48.60
Boat	0.22	49.20	0.20	48.60	0.20	48.63	0.26	48.75
Goldhill	0.16	48.90	0.15	48.50	0.15	48.50	0.24	48.50
Lena	0.22	49.20	0.21	48.80	0.21	48.68	0.38	49.05
Peppers	0.17	49.00	0.15	48.50	0.15	48.51	0.35	48.98
Zelda	0.22	49.20	0.19	48.60	0.20	48.61	0.27	48.77
Average	0.18	49.00	0.16	48.62	0.16	48.54	0.26	48.73

Table 7
Comparison of BPP, overflow, and PSNR of the medical images for the methods of Sachnev *et al.*,[11] Lee *et al.*,[15] and Zhao *et al.*[16] and the proposed method.

Medical image	Sachnev *et al.*[11]			Lee *et al.*[15]			Zhao *et al.*[16]			Proposed method		
	BPP	Overflow	PSNR	BPP	Overflow	PSNR	BPP	Overflow	PSNR	BPP	Overflow	PSNR
M1	0.00	0.73	53.47	0.00	0.73	49.59	0.40	0.34	56.14	0.66	0.06	52.26
M2	0.00	0.57	51.60	0.00	0.58	49.50	0.31	0.28	54.71	0.53	0.02	52.10
M3	0.00	0.56	51.53	0.00	0.56	45.70	0.35	0.28	54.66	0.10	0.01	59.87
M4	0.00	0.56	51.61	0.00	0.57	45.59	0.30	0.28	54.76	0.52	0.01	52.08
M5	0.16	0.23	49.21	0.16	0.23	49.77	0.34	0.12	52.33	0.22	0.00	57.83
M6	0.52	0.02	48.67	0.54	0.02	49.66	0.37	0.01	51.26	0.29	0.00	58.20
M7	0.00	0.28	49.14	0.00	0.28	49.12	0.20	0.14	52.60	0.24	0.00	52.86
M8	0.25	0.05	47.96	0.16	0.06	48.77	0.15	0.03	51.40	0.17	0.00	54.15
M9	0.55	0.00	48.55	0.59	0.00	49.63	0.39	0.00	51.14	0.30	0.00	57.95
Average	0.16	0.33	50.19	0.16	0.34	48.59	0.31	0.17	53.22	0.34	0.01	55.25

Table 8
BPP and PSNR of multilevel details and concealing contrasts of images of different methods.

Images	Lin and Hsueh[17]	Zeng *et al.*[4]	Li *et al.*[7]	Hsiao *et al.*[6]	Proposed method
Airplane	1.40	1.29	1.19	1.09	1.54
Baboon	0.61	0.49	0.55	0.53	0.87
Boat	1.17	1.05	0.86	1.02	1.21
Goldhill	1.16	N/A	0.90	0.94	1.23
Lena	1.18	1.07	1.15	1.16	1.60
Pepper	1.23	0.95	1.07	1.16	1.48
Tiffany	1.27	1.20	1.05	1.21	1.33
Average capacity	1.14	1.01	0.97	1.02	1.32
Average PSNR	30.26	30.34	30.00	30.02	30.05

In Table 8, multilevel details and concealing contrasts of the images are compared for different methods in terms of BPP and PSNR.[4,6,7,17] The results compare the amount of embedding (BPP) between the proposed method and other methods when PSNR is approximately equal to 30.

4.   Conclusions

We proposed an optimal prediction method based on the histogram shift method for reverse information hiding. Five prediction methods of the chessboard or column type were tested to obtain the optimized prediction algorithm. The chessboard-type methods showed better results than the column-type methods when testing for natural and CT medical images. When the hiding and extraction of image information of the optimized prediction method in this study were compared with those of previous methods, it was found that the proposed method generally showed better results for various images. The proposed algorithm hides and predicts images effectively, and is expected to be applied to WSNs because large amounts of image information are transmitted through WSNs.

References

1   R. Al-Sharif, C. Guyex, Y. A. Fadil, A. Makhoul, and A. Jaber: Proc. 2015 Int. Conf. Ad Hoc Networks (ADHOCNETS, 2015) 51. https://doi.org/10.1007/978-3-319-13329-4_5

2   D. M. Thodi and J. J. Rodriguez: IEEE Trans. Image Process. **16** (2007) 721. https://doi.org/10.1109/TIP.2006.891046

3   B. Ou, X. Li, Y. Zhao, R. Ni, and Y. Shi: IEEE Trans. Image Process. **22** (2013) 5010. https://doi.org/10.1109/TIP.2013.2281422

4   X-T. Zeng, L.-D. Ping, and Z. Li: J. Multimed. **4** (2009) 145. https://doi.org/10.4304/jmm.4.3.145-152

5   H.J. Kim, V. Sachnev, Y.Q. Shi, J. Nam, and H.-G. Choo: IEEE Trans. Inf. Forensics Secur. **3** (2008) 456. https://doi.org/10.1109/TIFS.2008.924600

6   J.-Y. Hsiao, K.-F. Chan, and J. M. Chang: Signal Process. **89** (2009) 556. https://doi.org/10.1016/j.sigpro.2008.10.018

7   Y.-C. Li, C.-M. Yeh, and C. C. Chang: Digit. Signal Process. **20** (2010) 1116. https://doi.org/10.1016/j.dsp.2009.10.025

8   O. M. Al-Qershi and B. E. Khoo: J. Syst. Softw. **84** (2011) 105. https://doi.org/10.1016/j.jss.2010.08.055

9   M. Liu, H.S. Seah, C. Zhu, W. Lin, and F. Tian: Signal Process. **92** (2012) 819. https://doi.org/10.1016/j.sigpro.2011.09.028

10   D. Hou, W. Zhang, Y. Yang, and N. Yu: IEEE Trans. Image Process. **27** (2018) 5087. https://doi.org/10.1109/TIP.2018.2851074

11   V. Sachnev, H. J. Kim, J. Nam, S. Suresh, and Y. Q. Shi: IEEE Trans. Circuits Syst. Video Technol. **19** (2009) 989. https://doi.org/10.1109/TCSVT.2009.2020257

12   Z. Ni, Y.-Q. Shi, N. Ansari, and W. Su: IEEE Trans. Circuits Syst. Video Technol. **16** (2006) 354. https://doi.org/10.1109/TCSVT.2006.869964

13   M. Fallahpour, D. Megias, and M. Ghanbari: Multimed. Tools Appl. **52** (2011) 513. https://doi.org/10.1007/s11042-010-0486-2

14   W.-L. Tai, C.-M. Yeh, and C. C. Chang: IEEE Trans. Circuits Syst. Video Technol. **19** (2009) 906. https://doi.org/10.1109/TCSVT.2009.2017409

15   C.-C. Lee, W.-H. Ku, and S.-Y. Huang: IET Image Process. **3** (2009) 243. https://doi.org/10.1049/IET-IPR.2008.0251

16   Z. Zhao, H. Luo, Z.-M. Lu, and J.-S. Pan: Int. J. Electron. Commun. **65** (2011) 814. https://doi.org/10.1016/j.aeue.2011.01.014

17   C-.C. Lin and N.-L. Hsueh: Pattern Recognit. **41** (2008) 1415. https://doi.org/10.1016/j.patcog.2007.09.005